



## OPEN Influence of pulverization on the micropore structure of coal and its fractal characteristics

Biao Hu<sup>1</sup>✉, Zeyu Ren<sup>1</sup>, Rongwei Luo<sup>1</sup>, Shugang Li<sup>1</sup>, Rong Zhang<sup>2</sup>, Hang Long<sup>1</sup> & Liang Cheng<sup>1</sup>

This study conducted extensive repetitive experiments by continuously adjusting the adsorption equilibrium judgement criteria to obtain reliable low-pressure CO<sub>2</sub> adsorption (LPGA-CO<sub>2</sub>) isotherms at 273 K for coal samples of different particle sizes. And the Horvath-Kawazoe (HK) model and density functional theory (DFT) were then employed to analyze the true evolution laws of micropore size distribution and its fractal characteristics in coal samples during the pulverization. It was found that constrained by the gas adsorption kinetics in large-particle coal samples, coal particles exceeding 0.3 mm are not recommended for porosity testing using LPGA-CO<sub>2</sub> (273 K). As coal particle size decreased from 0.3 mm to 0.075 mm, the most probable pore size in the micropore size distribution decreased, while micropore volume and surface area initially increased linearly. Below 0.075 mm, these parameters exhibited irregular, overall declining trends. These findings suggest that when the coal sample is crushed to a particle size below 0.075 mm, the internal closed pores are continuously opened, thereby promoting an increase in micropore volume. Concurrently, with increasing pulverization intensity, the micropore fractal dimension exhibited a linear rise from 2.029 to 2.337, demonstrating significantly enhanced surface roughness and spatial heterogeneity in micropores as coal particle size decreased.

**Keywords** Coal, Pulverization, Pores, Pore size distribution, Fractal characteristics

Coal, as a complex porous medium, possesses internal pore structures spanning from micrometer to molecular scales<sup>1,2</sup>. Previous research indicates that micropores dominate the pore structure of coal and serve as the primary storage space for coalbed methane<sup>3,4</sup>. Due to technical limitations, it remains challenging to directly and accurately determine the pore fracture structure and methane storage/migration characteristics in in-situ coal. Therefore, domestic and foreign scholars usually utilize small particle samples for alternative tests<sup>5</sup>. Characteristics derived from such particle samples are applied in on-site practice. For instance, China commonly employs the methane adsorption characteristics of coal samples with 0.18–0.25 mm particle size to describe the adsorption performance of in-situ coal. However, since particle pulverization significantly influences the sample's inherent properties<sup>6</sup>, investigating the dynamic evolution of micropore structure and its fractal characteristics during coal pulverization process is crucial for reproducing the true pore structure and properties of coal.

Various pore testing techniques have been employed in previous studies to describe the pore structure of coal particle samples, including field emission scanning electron microscopy (FE-SEM)<sup>2</sup>, scanning electron microscopy (SEM)<sup>7</sup>, atomic force microscopy (AFM)<sup>8</sup>, small-angle X-ray scattering (SAX)<sup>9</sup>, computed tomography (CT)<sup>10,11</sup>, mercury intrusion porosimetry (MIP)<sup>12</sup>, physical gas adsorption<sup>12,13</sup>, and nuclear magnetic resonance (NMR)<sup>14</sup>. Among them, MIP and physical gas adsorption are the most widely utilized. MIP is typically applied for characterizing macropore structures (> 50 nm) due to pore structural damage from elastic compression of coal at high pressures. Physical adsorption diverse gas adsorbates (argon, carbon dioxide, ethane, helium, krypton, methane, nitrogen, water vapor, xenon, etc.) are employed for quantitatively characterizing surface area, pore size distribution, and porosity of coal and other carbonaceous materials at lower cost and greater convenience than advanced techniques<sup>1</sup>. Among these, carbon dioxide (CO<sub>2</sub>) and nitrogen (N<sub>2</sub>) are the most prevalent gas adsorbates. Although CO<sub>2</sub> has a larger molecular diameter (0.387 nm) than N<sub>2</sub> (0.315 nm)<sup>15</sup>. The activation diffusion during the N<sub>2</sub> adsorption process at 77 K is limited by temperature, which delays gas permeation. In contrast, the thermal energy associated with CO<sub>2</sub> at 273 K is much greater<sup>16–20</sup>. (the diffusion rate of CO<sub>2</sub> at 273 K has been confirmed to be 105 times that of N<sub>2</sub> at 77 K)<sup>21</sup>. This indicates that the low-pressure

<sup>1</sup>School of Safety Science and Engineering, Xi'an University of Science and Technology, Xi'an 710054, Shaanxi, China. <sup>2</sup>Faculty of Safety Science and Engineering, Civil Aviation University of China, Tianjin 300300, China. ✉email: hubiao@xust.edu.cn

$N_2$  adsorption experiment is not ideal in quantitatively evaluating microporosity, especially for the size range of ultra-micropores (pore width less than 0.7 nanometers). Therefore, low-pressure  $CO_2$  adsorption (LPGA- $CO_2$ ) technology was often used to quantitatively characterize the micropore structure of particle coal samples in previous studies<sup>22</sup>.

However, scholars hold divergent views regarding whether pulverization affects the micropore structure of coal samples. Han et al.<sup>23</sup> contend that simple mechanical pulverization significantly impacts mesopore and macropore structures in coal but cannot disrupt nanoscale micropore structures. Conversely, Wang et al.<sup>24,25</sup> argue that the pulverization of coal samples alters their pore structure, leading to an increase in micropore and mesopore volumes, thereby enhancing their gas adsorption capacity. In a separate study, Wang et al.<sup>26</sup> investigated the complexity of pore structures in coal samples of varying particle sizes, finding that the pulverization process substantially influences the complexity of pore structure; specifically, pore structure tends to simplify as particle size decreases. Li et al.<sup>27</sup> examined the effects of coal particle size and temperature on the pore structure of low-rank coal, observing that micropore volume decreases with increasing treatment temperature when coal is pulverized at elevated temperatures. In our previous studies<sup>28,29</sup>, it has been found that using the same testing standards to characterize the pore structures of coal samples with different particle sizes can result in significant errors in the pore structure testing, often overestimating the impact of pulverization on the pore structure of coal samples.

In order to avoid the test errors caused by adsorption disequilibrium mentioned by scholars<sup>28,29</sup>, this study deeply analyzed the limitations of LPGA- $CO_2$  measurement, continuously refined the equilibrium judgment criteria for LPGA- $CO_2$  measurement. Extensive repetitive experiments were conducted on samples of varying particle sizes to obtain reliable equilibrium  $CO_2$  adsorption isotherms. Finally, under the prerequisite of ensuring accurate porosity testing, the influence of pulverization on the micropore distribution and fractal characteristics of coal samples was systematically analyzed. This study helps scholars to accurately obtain the micropore structures of coal samples with different particle sizes using LPGA- $CO_2$  (273 K) method, and to determine the influence of pulverization on the micropore structure of coal and its fractal characteristics.

## Sample preparation and experiments

### Coal sample preparation

In order to objectively evaluate the influence of coal pulverization on coal micropore structure and their fractal characteristics, fresh coal samples were taken from Working Face 21,070 of the No. 9–10 coal seam at Pingdingshan Coal Mine No. 8, Henan Province, China, following GB/T 19,222–2003. Fresh large pieces of coal samples were collected at the working face and packed into special sealed bags to prevent oxidation. After the coal samples were transported back to the laboratory, to avoid the impact of gangue and plastic impurities from on the subsequent test results, the coal samples were first subjected to secondary screening and then the screened coal samples were crushed. Finally, used a vibrating screen to screen the coal sample into samples of different particle size ranges, and put them into sealed bags respectively for future use. The particle size ranges of the samples were 1.0–2.0 mm, 0.5–1.0 mm, 0.3–0.5 mm, 0.2–0.3 mm, 0.125–0.2 mm, 0.075–0.125 mm, 0.045–0.075 mm and <0.045 mm respectively.

### Particle size distribution test

To facilitate quantitative analysis of the relationship between particle size and their pore structure/fractal characteristics of coal samples, particle size distribution was measured for samples across different particle size ranges using the Bettersize2600 laser particle size analyzer produced by Dandong Bettersize Instrument Co., Ltd. in accordance with the GB/T 19,077–2016 standard. To ensure the experimental data accuracy, the median particle size (D50) tests were repeated three times, with the average value recorded in Table 1 (Where  $M_{ad}$  denotes moisture content,  $A_d$  denotes ash yield,  $V_{daf}$  denotes volatile matter and  $FC_{ad}$  denotes fixed carbon). The picture of the testing equipment is shown in Fig. 1.

### Industrial analysis test

In accordance with the GB/T212-2008 standard, moisture, ash content, volatile matter, and fixed carbon were measured for coal samples of various particle sizes using the 5E-MAG6600 fully automatic industrial analyzer manufactured by Changsha Kaiyuan Instrument Co., Ltd. To ensure experimental data accuracy, the industrial analysis was repeated three times with average values obtained. The test results are shown in Table 1, and a

Particle size range (mm)	D50 (mm)	$M_{ad}$ (%)	$A_d$ (%)	$V_{daf}$ (%)	$FC_{ad}$ (%)
1.0–2.0	1.054 ± 0.021	0.80	18.57	29.34	57.08
0.5–1.0	0.631 ± 0.009	0.95	18.68	28.75	57.39
0.3–0.5	0.392 ± 0.012	0.89	17.49	28.69	58.32
0.2–0.3	0.270 ± 0.002	0.98	16.03	28.96	59.07
0.125–0.2	0.180 ± 0.004	1.05	15.36	29.01	59.45
0.075–0.125	0.106 ± 0.003	1.18	14.20	29.06	60.15
0.045–0.075	0.046 ± 0.002	1.18	14.06	28.73	60.53
<0.045	0.013 ± 0.001	1.28	13.86	28.59	60.73

**Table 1.** Basic parameters of coal samples with different particle sizes.

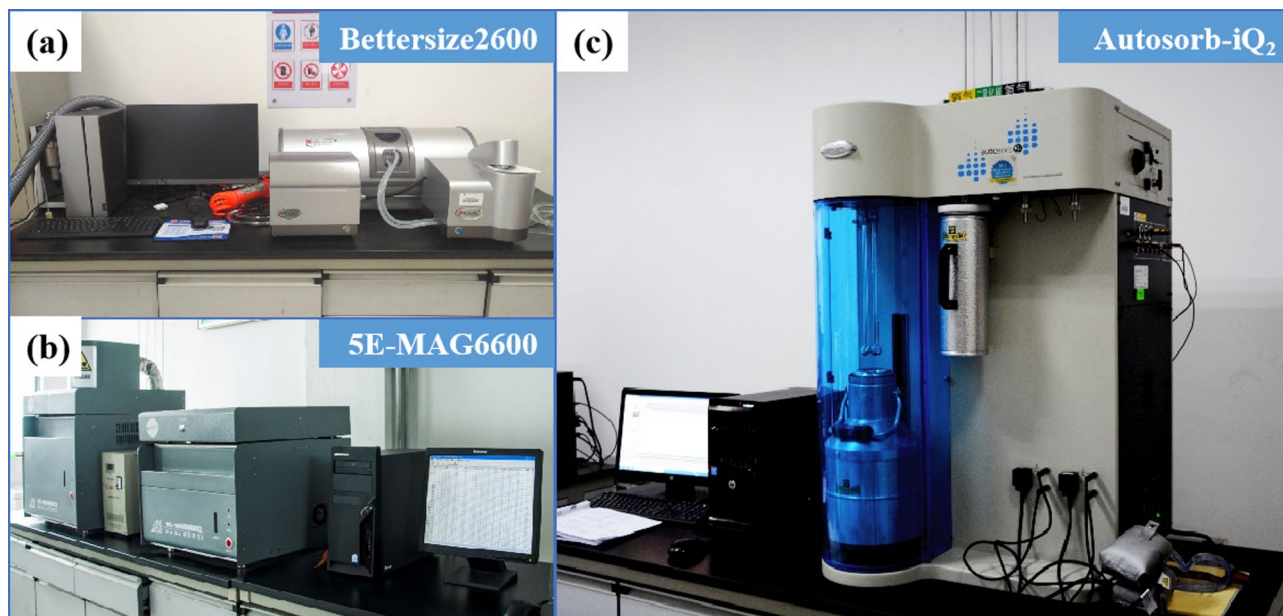


**Fig. 1.** Images of the experimental apparatus: (a) Bettersize2600 laser particle size analyzer; (b) 5E-MAG6600 automatic proximate analyzer; (c) Autosorb-iQ<sub>2</sub> Automated Gas Sorption Analyzer.

photograph of the testing equipment is presented in Fig. 1. Based on industrial analysis of coal samples with varying particle sizes (Table 1), significant variations in fundamental parameters are observed even within the same coal sample. Moisture content exhibits a pronounced increasing trend with decreasing particle size, rising from 0.80% to 1.28%. This result aligns with the test results of Jin et al.<sup>30</sup>, speculating that the pulverization of coal samples leads to varying degrees of enhanced pore development, resulting in the inherent moisture content of small-particle coal samples being higher than that of large-particle coal samples. Ash content of coal samples demonstrates a marked increase with larger particle size, climbing from 13.86% to 18.68%. A similar trend reported by Cloke et al.<sup>28,31</sup> is speculated to result from incomplete high-temperature combustion for an insufficient period of time within larger particles during ashing, where unburned combustible matter is erroneously measured as ash, yielding elevated values. Fixed carbon content shows a significant rise with decreasing particle size. This can be likewise attributed to incomplete volatile matter release for an insufficient period of time during industrial analysis, causing anomalously high volatile readings in larger particles<sup>28</sup>. Volatile matter content shows no clear correlation with particle size. Collectively, these findings indicate that after the coal sample is crushed and sieved, there are certain alterations in industrial analysis components, including moisture, ash, volatile matter, fixed carbon, may be attributable to the crushing process, the sieving process and the industrial analysis experiment process of the coal sample.

### LPGA-CO<sub>2</sub> test

To quantitatively investigate the impact of coal pulverization on its internal pore structure and fractal characteristics, this study employed LPGA-CO<sub>2</sub> (273 K) to characterize the micropore structure. The LPGA-CO<sub>2</sub> (273 K) tests were conducted using an Autosorb-iQ<sub>2</sub> automated gas sorption analyzer (Fig. 1) produced by Quantachrome Instruments, USA, the test and data processing & analysis were carried out according to GB/T 21650.3–2008/ISO 15901-3:2006. Prior to testing, samples were pre-dried (323 K, 48 h) to prevent damage to the spiral molecular pump of physical adsorption instrument by residual moisture. Samples were degassed at 373 K for 10 h in the degas station to remove gases, moisture, and other impurities in the samples at the beginning of the experiment. Subsequently, the sample tube was transferred to the analysis station and immersed in a 273.15 K ice-water bath. Adsorption data were collected within the range of relative pressure of  $3 \times 10^{-5}$  to 0.0289 (the value of CO<sub>2</sub> saturated vapor pressure at 273 K in the analysis software was 26,200 torr, about 3.496 MPa)<sup>32</sup>. In the setting of experimental equilibrium determination parameters (time interval), in order to ensure that the CO<sub>2</sub> adsorption of different coal samples reached complete equilibrium, the experimental adsorption equilibrium determination time was continuously revised<sup>28,29</sup> until the same adsorption isothermal line was obtained under different experimental equilibrium determination parameters (time interval). This indicated successful completion of the repeatability test, with the resulting LPGA-CO<sub>2</sub> adsorption isotherm at 273 K being designated as the final reference. To conserve resources, the final equilibrium adsorption isotherms for ultra-large particle size samples were not measured.

## Results and analysis

### LPGA-CO<sub>2</sub> adsorption isotherms

Previous studies by Mastalerz et al.<sup>28,33–36</sup> found that large-particle coal samples were difficult to reach gas adsorption equilibrium, concluding that the physical adsorption method was unsuitable for characterizing large-

particle coal samples' pore structures. Moreover, comparing the isothermal data under adsorption equilibrium and non-equilibrium conditions of large-particle coal samples revealed that adsorption disequilibrium had a significant impact on pore structure characterization<sup>29</sup>. To investigate the interrelationship among the particle size, micropore structure and adsorption characteristics of coal samples, extensive repetitive experiments were conducted in this study, continuously changing the equilibrium judgment time during the adsorption test process. Finally, the LPGA-CO<sub>2</sub> (273 K) adsorption isotherms of 21070Y coal samples with different particle sizes were obtained, as shown in Fig. 2. When testing the LPGA-CO<sub>2</sub> (273 K) adsorption data of the 21070Y coal sample with a particle size of 0.3–0.5 mm, the adsorption equilibrium judgment time was set to 12 min, resulting in a total adsorption test duration of approximately 3560 min. Considering factors such as test reliability, time and cost, the LPGA-CO<sub>2</sub> (273 K) adsorption data of coal samples larger than 0.5 mm were not subjected to repetitive testing.

Analysis of the LPGA-CO<sub>2</sub> (273 K) adsorption curves for different particle sizes of the 21070Y coal sample (Fig. 2) reveals that the adsorption isotherms for particles larger than 0.5 mm exhibit a distinct linear trend with increasing pressure, whereas those for smaller particles tend to follow a Langmuir-type trend. At a relative pressure of 0.0289, the CO<sub>2</sub> adsorption capacity of the 21070Y coal sample increases from 4.658 cm<sup>3</sup>/g to 10.997 cm<sup>3</sup>/g (2.36 times) as particle size decreases. However, for coal particle below 0.3 mm, the CO<sub>2</sub> adsorption capacity of the 21070Y coal sample rises by only 9.2%. This indicates that the near-linear adsorption isotherms observed for large-particle coal samples of the LPGA-CO<sub>2</sub> (273 K) test result from adsorption disequilibrium, which significantly impacts the quantitative characterization of the micropore structure in coal<sup>29</sup>. Therefore, when utilizing the LPGA-CO<sub>2</sub> (273 K) adsorption method to characterize the micropore structure of coal, it is recommended that the selected coal particle size should not exceed 0.3 mm<sup>29,36</sup>.

### Pore size distribution of micropores

The commonly used data analysis methods for the LPGA-CO<sub>2</sub> (273 K) isothermal adsorption data mainly include the Dubinin-Astakhov method (DA method)<sup>37</sup>, the Horvath-Kawazoe method (HK method)<sup>38,39</sup>, the Saito-Foley method (SF method)<sup>40,41</sup>, the Monte-Carlo molecular simulation method (MC method)<sup>42,43</sup> and the density functional theory (DFT) method. For instance, Hu et al.<sup>28</sup> processed the LPGA-CO<sub>2</sub> (273 K) isothermal adsorption data of the same coal sample using different data analysis methods and obtained the pore size distribution characteristics, as shown in Fig. 3.

Figure 3 presents the pore size distribution characteristics of micropores in coal sample obtained using five analytical methods: DA, HK, SF, DFT and MC. Comparison reveals that the DA method exhibits the broadest analysis range (0.02–6.0 nm), while the HK method has the narrowest range (only 0.3–0.6 nm). The SF method covers a range of 0.31–1.05 nm. The DFT and MC methods share an identical pore size distribution range (0.3–1.47 nm) and demonstrate strong consistency across this entire range. At the same time, both methods show excellent agreement with the HK method when analyzing the pore structure of ultra-micropores smaller than 0.6 nm<sup>28</sup>. Considering the applicability and analysis ranges of these methods, this study ultimately employed the DFT and HK methods to process the LPGA-CO<sub>2</sub> (273 K) adsorption isotherm data. The DFT method was selected as the primary tool for its robust theoretical basis and its ability to provide accurate quantitative parameters across the entire micropore range. However, we observed that the data points of the pore size distribution curves generated by DFT in the ultra-micropore region (< 0.7 nm) are too scattered to precisely resolve the distribution peaks. Therefore, to better characterize the subtle changes in the most probable pore size, the HK method was adopted as a supplementary means. The HK method can generate a more continuous curve in this narrow range, facilitating a clearer comparative analysis of the distribution characteristics of ultra-micropores. To facilitate comparison of the particle size effect on pore structure and to exclude interference

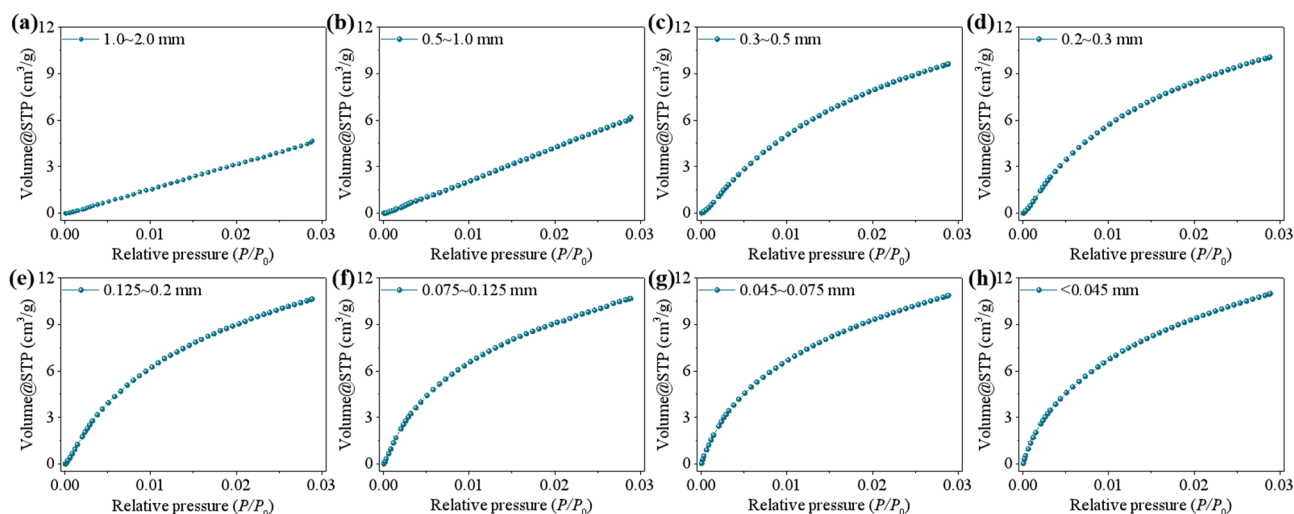


**Fig. 2.** LPGA-CO<sub>2</sub> (273 K) adsorption isotherms of coal samples with different particle sizes.

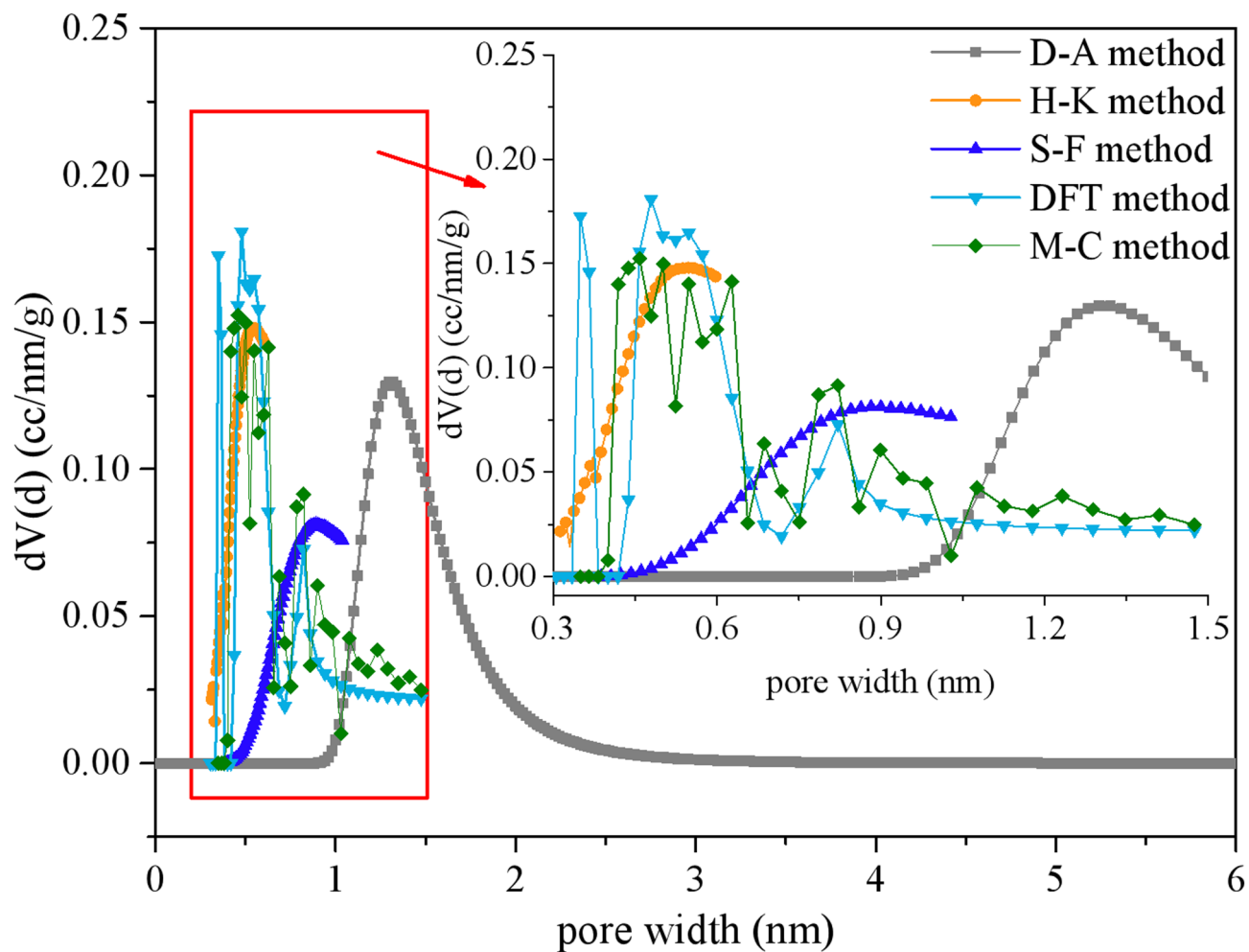


**Fig. 3.** Comparison of pore size distribution of low-pressure CO<sub>2</sub> (273 K) adsorption isotherms by different data analysis methods<sup>28</sup>.

from disequilibrium adsorption data, the cumulative pore volume distribution characteristics for 21070Y coal samples with particle sizes less than 0.5 mm were compared, as shown in Fig. 4. The fitting errors for the DFT method were consistently below 1%, indicating good data reliability.

Within the pore size range of 0.3–0.45 nm, the cumulative pore volume distribution curves rise with decreasing coal particle size. However, when the pore size increases to approximately 0.6 nm, the cumulative pore volume distribution curves almost overlap, indicating that the cumulative pore volumes of 21070Y coal samples with different particle sizes are almost the same within the range of 0.3 to 0.6 nm. Due to the overly discrete data points of the pore size distribution curves obtained using the DFT method for analyzing ultra-micropores (< 0.7 nm), the HK method is employed to comparatively analyze the ultra-micropore pore size distribution laws of the 21070Y coal samples. The volume distribution curves of 21070Y coal samples with different particle sizes within the 0.3–0.6 nm range increase gradually with pore size, reach a peak of the pore size distribution curve, and then decline. Comparison reveals that the most probable pore size at the peak of the pore size distribution curve is closely related to the coal sample and its particle size. Pore size distribution for large-particle coal samples exhibit a faster growth rate and a more significant decay after the peak point. This phenomenon may be attributed to the following reasons: (1) The abundant ultra-micropore structure in small coal particles may be newly generated during coal sample crushing process, resulting from the destruction of pore structures within the 0.45–0.6 nm range. (2) Small-particle coal samples contain numerous closed pores at the ultra-microporous scale. During the particle crushing process, the structural weak surfaces within the closed pores are damaged, which leads to the continuous opening of the closed pores and causes the ultra-micropores to increase as the particle size decreases. (3) pulverization itself may not affect ultra-micropores, but the diffusion path of micropores in large-particle coal samples is relatively long, which leads to insufficient filling of micropores during the pore testing process. Gas molecules that should have been adsorbed at lower relative pressures are transferred to higher relative pressures, thereby introducing bias into the pore analysis results<sup>29,36</sup>.

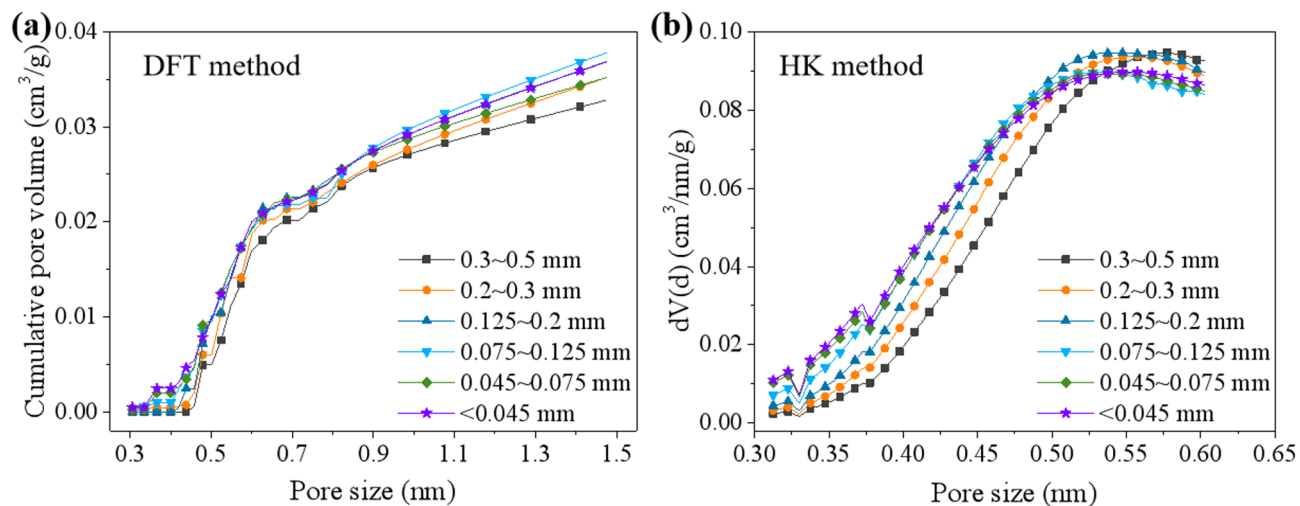


**Fig. 4.** Variation of pore with coal particle size: (a) cumulative micropore volumes (DFT method); (b) volume distribution of ultra-micropores (HK method).

### Fractal features of micropore structures

The LPGA-CO<sub>2</sub> (273 K) adsorption method is based on the adsorption behavior of CO<sub>2</sub> molecules at 273 K to characterize the micropore structure of coal samples. To quantify the geometric complexity of the micropore structure, a fractal dimension analysis was performed on the adsorption data. The selection of an appropriate fractal model is crucial and depends on the underlying physical adsorption mechanism. For instance, the Frenkel-Halsey-Hill (FHH) model is widely used for multilayer adsorption, often applied to N<sub>2</sub> adsorption isotherms. However, low-pressure CO<sub>2</sub> adsorption at 273 K is dominated by micropore volume filling rather than surface layering. Consequently, a model based on the principles of micropore filling is more suitable for characterizing the geometric complexity of the micropore network. The Sierpinski model, as adapted for gas adsorption, provides such a framework. The Sierpinski fractal method describes the relationship between the typical fractal volume  $V$  embedded in three-dimensional space and the characteristic measurement scale  $L$  as:

$$V = L^{(3-D_{SIE})} \quad (1)$$

Where  $D_{SIE}$  is volume fractal dimension.

On this basis, Angulo et al.<sup>44</sup> argued that the LPGA-CO<sub>2</sub> process is not a box-counting process of Sierpinski fractal dimension, and modified Eq. (1) to a relationship between volume and pressure:

$$V \propto (p - p_t)^{(3-D_{SIE})} \quad (2)$$

Where  $V$  is the volume of CO<sub>2</sub> adsorbed at equilibrium pressure  $p$ ;  $p_t$  is the threshold pressure, for the isothermal adsorption experiment of LPGA-CO<sub>2</sub> (273 K), the pressure value of the first adsorption data point on the isothermal adsorption curve is usually taken.

Taking the logarithm of both ends of Eq. (2):

$$\ln V = c + (3 - D_{SIE}) \ln (p - p_t) \quad (3)$$

During the CO<sub>2</sub> adsorption process at 273 K, CO<sub>2</sub> molecules are adsorbed in the form of micropore filling in the micropore structure. To ensure the reliability of the fractal data, the CO<sub>2</sub> adsorption data with a relative pressure less than 0.02 is selected for analysis. The LPGA-CO<sub>2</sub> (273 K) adsorption data measured by different particle sizes of 21070Y coal samples were brought into Eq. (3), plot with  $\ln(p-p_t)$  as the abscissa and  $\ln(V)$  as the ordinate, as shown in Fig. 5.

The volumetric fractal dimension  $D_{SIE}$  of 21070Y coal samples across varying particle sizes ranges from 1.786 to 2.337, exceeding the normal range of the fractal dimension (2~3). Moreover, the samples that exceed the value range are all from large-particle coal samples. Coupled with the LPGA-CO<sub>2</sub> (273 K) isotherms of the 21070Y coal samples with different particle sizes shown in Fig. 2, it is speculated that the LPGA-CO<sub>2</sub> (273 K) isotherm adsorption data of the large-particle coal samples are non-equilibrium data and cannot accurately characterize the micropore structure of the coal samples<sup>29,36</sup>. Therefore, the fractal dimension values  $D_{SIE}$  derived from coal samples with particles sizes exceeding 0.3 mm fall below 2 due to data distortion, suggesting that such  $D_{SIE}$  results for large-particle coal samples may be meaningless. To avoid the influence of non-equilibrium adsorption data on the characterization of pore structure, comparison of  $D_{SIE}$  in sub-0.3 mm coal samples reveals that when the particle size of the coal sample decreases from 0.3 mm to < 0.045 mm, the  $D_{SIE}$  of the 21070Y coal sample rises linearly from 2.029 to 2.337 (+ 15.2%) indicating an increase in the surface roughness and tortuosity of the micropores. This changing trend aligns with the volume and specific surface area of coal samples' micropores

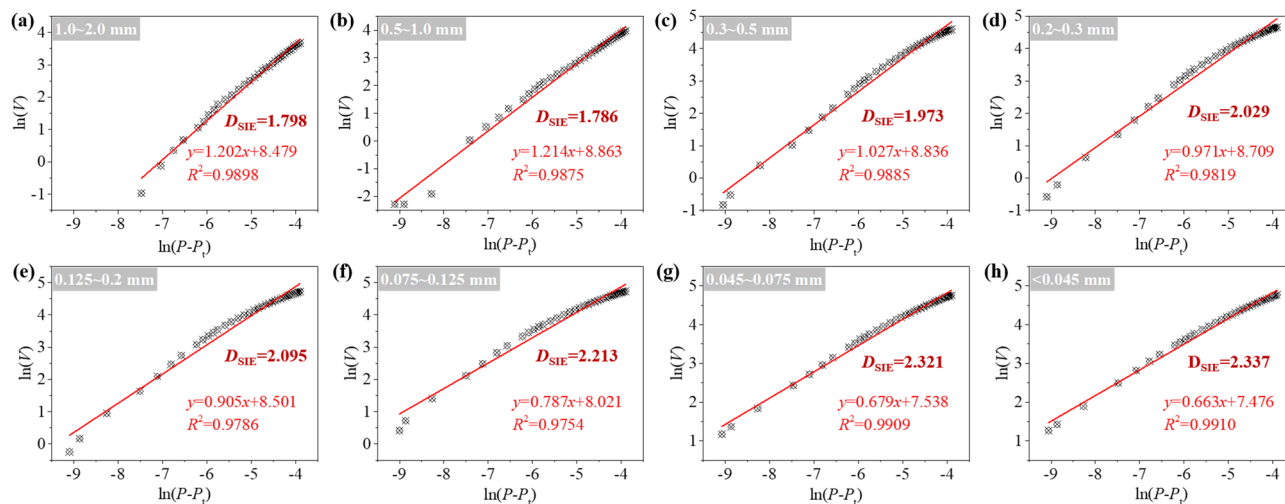


**Fig. 5.** Fractal fitting curve of the low-pressure CO<sub>2</sub> (273 K) adsorption data of 21070Y coal samples with different particle sizes.

Particle size range (mm)	Pore size distribution		Fractal dimension	
	PV (cm <sup>3</sup> /g)	SSA (m <sup>2</sup> /g)	$D_{SIE}$	$R^2$
0.3–0.5	0.033	99.151	1.973	0.9885
0.2–0.3	0.035	107.260	2.029	0.9819
0.125–0.2	0.037	113.248	2.095	0.9786
0.075–0.125	0.038	117.418	2.213	0.9754
0.045–0.075	0.035	113.978	2.321	0.9909
<0.045	0.037	117.493	2.337	0.9910

**Table 2.** Results of pore volume and specific surface area of 21070Y coal samples with different particle sizes.

with different particle sizes in Sect. 3.2, demonstrating that as the particle size decreases, the internal micropore structure gradually increases, and the internal pore network becomes more complex. It is speculated that coal pulverization likely opens a large number of closed pores inside the coal, thereby increasing the number of micropores and elevating fractal dimensions.

### The influence of pulverization on the coal pore structures

The LPGA-CO<sub>2</sub> (273 K) adsorption isotherm data of the coal samples were analyzed using the DFT method. The total pore volume and specific surface area of the micropore pore structures within the 0.33–1.5 nm range for different particle sizes of the 21070Y coal sample were summarized in Table 2. Meanwhile, the volume fractal dimension ( $D_{SIE}$ ) was calculated based on the slope of the fractal fitting curves described in Sect. 3.3, and the fractal dimension results were also compiled in Table 2. Based on the fractal dimension calculation results for the 0.3–0.5 mm coal samples, it was judged that the LPGA-CO<sub>2</sub> (273 K) isothermal adsorption data for coal samples with particle sizes above 0.3 mm were likely disequilibrium data. Therefore, the micropore volume, specific surface area, and fractal dimension of the coal samples with particle size less than 0.3 mm were analyzed. The variation of pore characteristic parameters of micropores with median particle size during the crushing process is presented in Fig. 6.

Figure 6 shows that as the particle size of coal sample decreases from 0.2 to 0.3 mm ( $D_{50} = 0.270$  mm) to < 0.045 mm ( $D_{50} = 0.013$  mm), the micropore volume of coal sample rapidly increases from 0.035 cm<sup>3</sup>/g to 0.038 cm<sup>3</sup>/g and then slowly reduces to 0.037 cm<sup>3</sup>/g. The specific surface area of micropores rapidly increases from 107.260 m<sup>2</sup>/g to 117.418 m<sup>2</sup>/g and then slowly rises to 117.493 m<sup>2</sup>/g, while the micropore fractal dimension increases linearly from 2.029 to 2.337. Comparing the changes of micropore volume, specific surface area and fractal dimension of 0.075–0.2 mm particle size with the particle size of the coal sample reveals a relatively stable impact of coal pulverization on the micropore structure of 21070Y, with these parameters basically increasing linearly as particle size decreases. It is speculated that when the mechanical destruction reaches a particle size of 0.075 mm, the closed pores inside the coal sample are continuously opened, thereby promoting the growth of the micropore structure. However, for sizes below 0.075 mm, both the microporous pore volume and specific surface area decrease to a certain extent with decreasing particle size, exhibiting no clear variation trend. It is speculated that when the particle size of the coal sample is mechanically damaged to below 0.075 mm, the internal pores are damaged, thereby promoting the collapse of the micropore structure<sup>28,29,36</sup>. Combined with

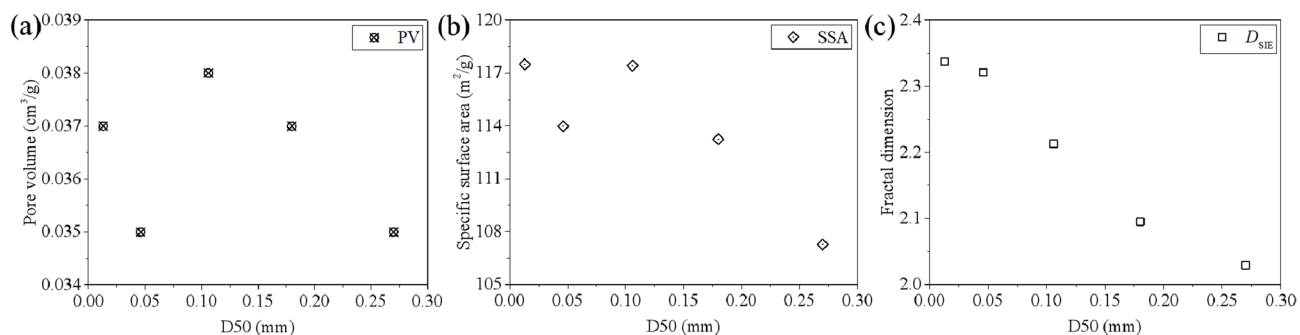


**Fig. 6.** The relationships between the median particle size of coal samples and their pore volume, specific surface area, and fractal dimension.

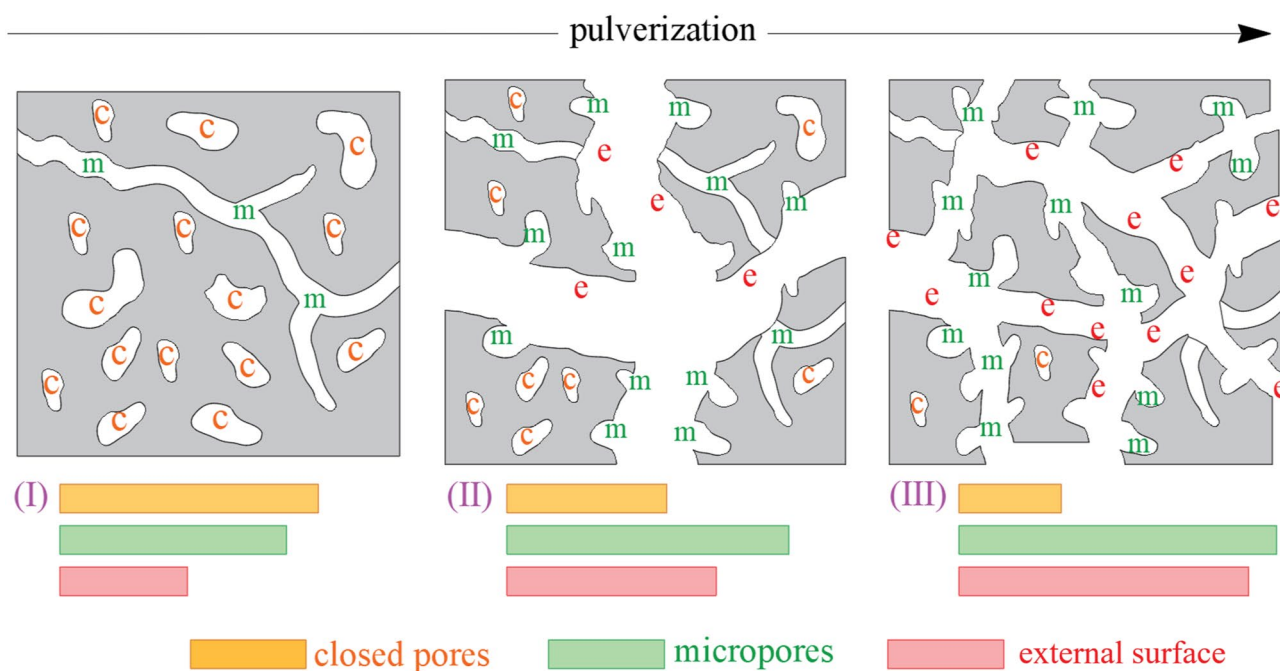


**Fig. 7.** Schematic diagram of microporous structure evolution during coal pulverization process. (The letter “c” denotes closed pores, the letter “m” represents micropores, and the letter “e” indicates the external surface.)

the variation law of macropore structure with particle size in coal samples by other scholars during the coal crushing process, it can be found that the mesoporous pore volume and specific surface area inside the coal particles increase rapidly with decreasing particle size, with an increase range of 348.2%~501.3%. This indicates that coal pulverization has a significant impact on the coal pore structure<sup>45</sup>, inevitably leading to drastic changes in the occurrence and migration characteristics of gas in coal. Schematic diagram of microporous structure evolution during coal pulverization process is shown in Fig. 7, which can be divided into three stages: (I) a large coal particle contains a network of accessible micropores (m), a limited external surface (e), and numerous inaccessible closed pores (c); (II) moderate pulverization breaks the particle, creating new external surfaces and opening some closed pores, which become part of the accessible micropore network, thus increasing the total measurable micropore volume; (III) intensive pulverization to very fine sizes continues to open closed pores but may also cause mechanical damage and collapse of the delicate pore walls, potentially leading to a stabilization or slight decrease in the overall micropore volume, as observed for particles smaller than 0.075 mm.

The pore structure in coal, as a typical fractal geometry, exhibits a fractal dimension that partially reflects the roughness and complexity of the pore structures. Therefore, a correlation analysis is conducted between the fractal dimension of coal samples with a particle size of less than 0.3 mm and their pore volume / specific surface area. The relationship between the volume fractal dimension  $D_{SIE}$  obtained based on the adsorption data of LPGA-CO<sub>2</sub> (273 K) and the pore volume / specific surface area is shown in Fig. 8.

It can be known from Fig. 8 that the fractal dimension  $D_{SIE}$  of micropores and the pore volume of coal samples with particle size less than 0.3 mm show irregular changes, while the change between  $D_{SIE}$  and the specific surface area shows a certain law. The least square method is used to fit the relationship between the

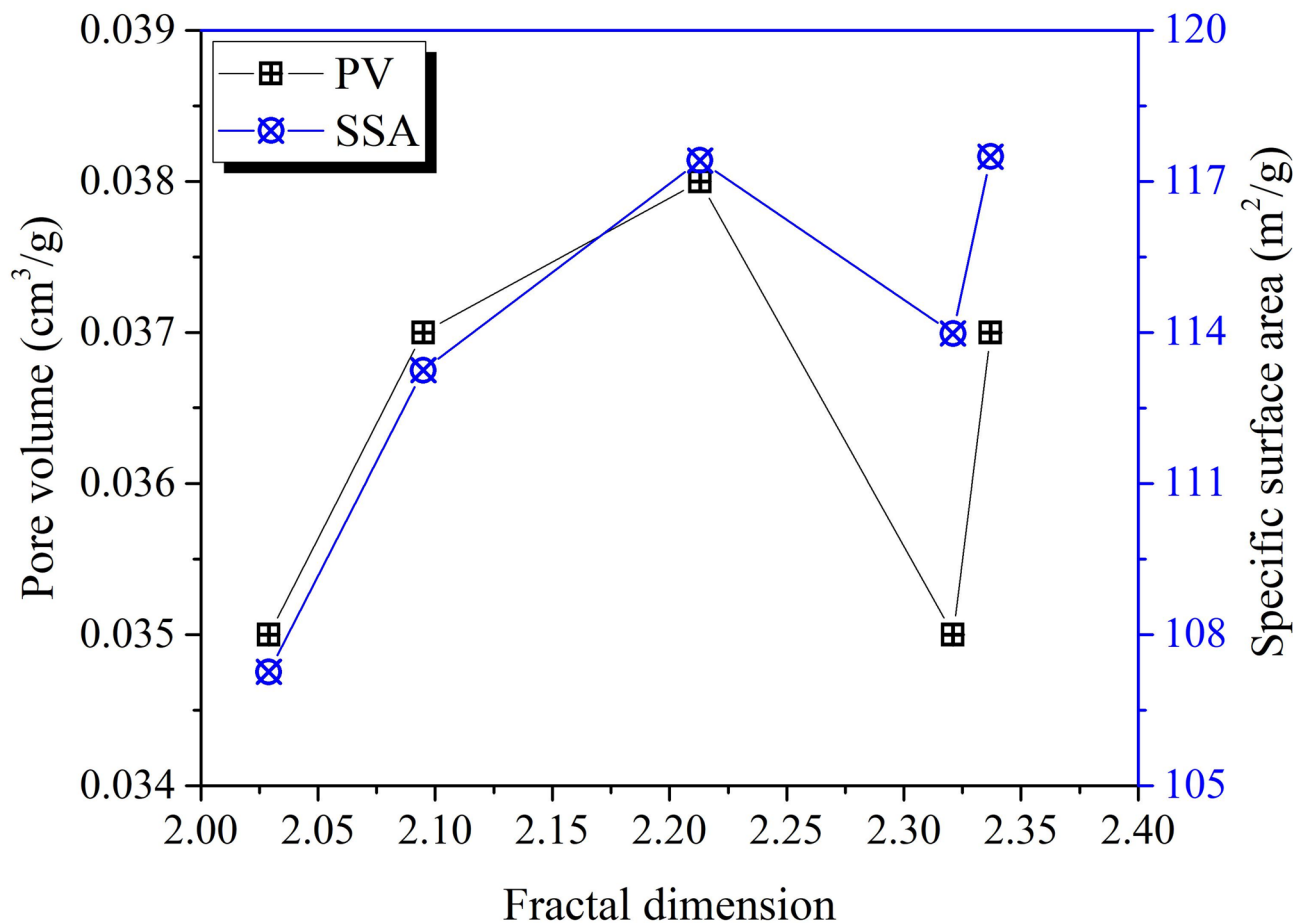


**Fig. 8.** Relationship between fractal dimension  $D_{SIE}$  and the pore volume / specific surface area.

fractal dimension of micropores and the specific surface area, indicating that there is a positive correlation between the two ( $SSA = 23.716D_{SIE} + 61.727$ ,  $R^2 = 0.5950$ ). It manifests that the finer the coal sample particles are, the more complex the surface of the micropores is, which is consistent with the conclusion proposed by Hao et al. that “the surface area of the micropores dominates the fractal dimension”.

It should be noted that the coal samples employed in this study are medium-rank coal. The pore testing technique adopted is only LPGA- $\text{CO}_2$  to characterize micropores, without using alternative fractal theories to analyze micropore fractal characteristics. Therefore, it is possible to consider preparing more coal samples with varying metamorphic degrees and utilize more testing methods to analyze their pore structures in the future, such as SANS or FIB-SEM to analyze the changes in micropore characteristics, apply diverse fractal theories to conduct deeper investigations into their fractal properties.

## Conclusions

This study employs a rigorous methodology to ensure the attainment of true adsorption equilibrium, providing a more reliable dataset to address existing controversies regarding the impact of pulverization on coal micropores in previous research. It enables scholars to accurately characterize the micropore structure of coal samples with different particle sizes using the LPGA- $\text{CO}_2$  (273 K) method, and to determine the effects of pulverization on both the micropore structure and fractal characteristics of coal.

- (1) For coal samples with particle sizes exceeding 0.3 mm, the LPGA- $\text{CO}_2$  (273 K) adsorption test duration of over 3560 min, and the measured data cannot guarantee adsorption equilibrium. Therefore, it is not recommended that the particle size of coal samples exceed 0.3 mm when using the LPGA- $\text{CO}_2$  (273 K) adsorption method to test the porosity of coal samples;
- (2) Micropore size distribution of coal samples with different particle sizes increases gradually with pore size, reach a peak of the pore size distribution, and then decline. Comparison reveals that the most probable pore size at the peak of the pore size distribution curve is closely related to the coal sample and its particle size. Micropore size distribution for large-particle coal samples exhibit a faster growth rate and a more significant decay after the peak point;

- (3) For coal samples with particle size ranges from 0.075 to 0.2 mm, the micropore volume, specific surface area and fractal dimension with the particle size of the coal sample basically increasing linearly as particle size decreases, revealing that when coal pulverization reaches a particle size of 0.075 mm, the closed pores inside the coal sample are continuously opened, thereby promoting the growth of the micropore structure. For sizes below 0.075 mm, both the microporous pore volume and specific surface area decrease to a certain extent with decreasing particle size, exhibiting no clear variation trend. This is likely due to the partial collapse or merging of some micropores caused by intensive mechanical damage;
- (4) With the decrease of particle size, the fractal dimension  $D_{SIE}$  of the pore system of the coal sample shows a regular increase, rising linearly from 2.029 at 0.3 mm to 2.337 at <0.045 mm (an increase of 15.2%), indicating that with the increase of pulverization degree, the pore surface roughness and spatial heterogeneity of micropores are significantly enhanced.

### Data availability

The original contributions presented in this study are included in the article, further inquiries can be directed to the corresponding author.

Received: 8 August 2025; Accepted: 25 November 2025

Published online: 12 December 2025

### References

1. Gregory, N., Okolo, R. C., Everson, Hein, W. J. P., Neomagus, M. J. & Roberts, R. Comparing the porosity and surface areas of coal as measured by gas adsorption, mercury intrusion and SAXS techniques[J]. *Fuel* **141**, 293–304. <https://doi.org/10.1016/j.fuel.2014.10.046> (2015).
2. Qu, Y. et al. Fractal characterization of a multi-scale pore structure in ultra-deep coal seams[J]. *Fractal Fract.* **9** (4), 250. <https://doi.org/10.3390/fractalfract9040250> (2025).
3. Yuanping, C. & Biao, H. Main occurrence form of methane in coal: micropore filling[J]. *J. China Coal Soc.* **46** (9), 2933–2948. <https://doi.org/10.13225/j.cnki.jccs.2020.1214> (2021).
4. Hu, B. et al. A new quantitative characterization method of absolute methane adsorption isotherm in coal. *Chem. Eng. J.* **522**, 167551. <https://doi.org/10.1016/j.cej.2025.167551> (2025).
5. He, X. et al. Co-Evolution of specific stiffness and permeability of rock fractures offset in Shear[J]. *J. Geophys. Research: Solid Earth.* **130** (5), 1–19. <https://doi.org/10.1029/2024JB030633> (2025).
6. He Xinxin, E., Derek, L. & Shimin Millisecond-resolved gas sorption kinetics and time-dependent diffusivity of coal[J]. *Rock Mech. Rock Eng.* **58** (4), 4421–4439. <https://doi.org/10.1007/s00603-024-03952-0> (2025).
7. Huang, Y. et al. Pyrolysis behaviors of lump sub-bituminous coal. Part 1: structural evolution of Chars both at particle surface and center[J]. *Fuel* **376**, 132709. <https://doi.org/10.1016/j.fuel.2024.132709> (2024).
8. Li, Y. et al. Microstructural response of coal fracture surface induced by ScCO<sub>2</sub> injection measured with AFM[J]. *Gas Sci. Eng.* **131**, 205471. <https://doi.org/10.1016/j.jgsce.2024.205471> (2024).
9. He Xinxin, Z., Rui, D., Elsworth, L., He, S. & Liu Beyond liquid density assumptions: A novel SANS-based approach to quantify adsorbed methane and adsorption-induced coal microstructure alterations[J]. *Chem. Eng. J.* **518**, 164725. <https://doi.org/10.1016/j.cej.2025.164725> (2025).
10. Chen Xuexi, M., Ruiyue, W., Jinsui, S. & Jihong Fractal analysis of coal pore structure based on computed tomography and fluid intrusions[J]. *Fractal Fract.* **7** (6), 439. <https://doi.org/10.3390/fractalfract7060439> (2023).
11. Zhang Na, W., Shuaidong, W., Jiaqi, L. & Zheng, W. Full-scale pore structure characterization and its impact on methane adsorption capacity and seepage capability: differences between shallow and deep coal from the Tiefa basin in Northeastern China[J]. *Fractal Fract.* **8** (1), 48. <https://doi.org/10.3390/fractalfract8010048> (2024).
12. Wang, S. et al. Multifractal characterization of pore structure of coals using gas adsorption experiment and mercury intrusion porosimetry (MIP)[J]. *Fractal Fract.* **9** (3), 183. <https://doi.org/10.3390/fractalfract9030183> (2025).
13. Feng, K. et al. Fractal strategy for improving characterization of N<sub>2</sub> adsorption–desorption in mesopores[J]. *Fractal Fract.* **8** (11), 617. <https://doi.org/10.3390/fractalfract8110617> (2024).
14. Lin Wei, Z., Xinli, L., Mingtao, Y. & Zhuang Pore structure characterization and fractal characteristics of tight limestone based on low-temperature nitrogen adsorption and nuclear magnetic resonance[J]. *Fractal Fract.* **8** (7), 371. <https://doi.org/10.3390/fractalfract8070371> (2024).
15. Sondergeld, C. H., Newsham, K. E., Comisky, J. T., Rice, M. C. & Rai, C. S. February. Petrophysical considerations in evaluating and producing shale gas resources[C]. *SPE Unconventional Gas Conference*, (Pittsburgh, Pennsylvania, USA, 2010). <https://doi.org/10.2118/131768-MS>
16. Gökhan Şenel, İ., Güniz Gürüz, A., Yücel, H., Kandas, A. W. & Adel, F. Sarofim. Characterization of pore structure of Turkish coals[J]. *Energy Fuels.* **15** (2), 331–338. <https://doi.org/10.1021/ef000081k> (2001).
17. Mahajan, O. P. CO<sub>2</sub> surface area of coals: the 25-year paradox[J]. *Carbon* **29** (6), 735–742. [https://doi.org/10.1016/0008-6223\(91\)90010-G](https://doi.org/10.1016/0008-6223(91)90010-G) (1991).
18. Mastalerz Maria, H., Lilin, M., Yuri, B. & Rupp John, A. Porosity of coal and shale: insights from gas adsorption and SANS/USANS techniques[J]. *Energy Fuels.* **26** (8), 5109–5120. <https://doi.org/10.1021/ef300735t> (2012).
19. Radovic, L. R. et al. On the porous structure of coals: evidence for an interconnected but constricted micropore system and implications for coalbed methane recovery[J]. *Adsorption* **3** (3), 221–232. <https://doi.org/10.1007/BF01650133> (1997).
20. Mahajan, O. P. Physical characterization of coal[J]. *Powder Technol.* **40** (1–3), 1–15. [https://doi.org/10.1016/0032-5910\(84\)85052-4](https://doi.org/10.1016/0032-5910(84)85052-4) (1984).
21. Thomas Josephus, Damberger, H. H. Internal surface area, moisture content, and porosity of Illinois coals: variations with coal rank[J]. *Urbana: Ill. State Geol. Surv.* **493**, 40 (1976). <https://hdl.handle.net/2142/43027>
22. Hu, B. et al. The distribution characteristics of adsorbed CH<sub>4</sub> in various-sized pore structures of coal seams. *Mathematics* **13** (18), 2931. <https://doi.org/10.3390/math13182931> (2025).
23. Han, H. et al. Influence of particle size on gas-adsorption experiments of shales: an example from a longmaxi shale sample from the Sichuan Basin, China[J]. *Fuel* **186**, 750–757. <https://doi.org/10.1016/j.fuel.2016.09.018> (2016).
24. Wang, J. et al. Post-outburst coal pulverization: experimental insights with representative accident samples[J]. *Energy Sour. Part A Recover. Utilization Environ. Eff.* **46** (1), 11413–11434. <https://doi.org/10.1080/15567036.2024.2387829> (2024).
25. Li, X. et al. Nanopore characterization related to particle size during coal pulverization: insights from cryogenic N<sub>2</sub> adsorption experiments[J]. *Int. J. Coal Preparation Utilization.* **45** (8), 1715–1736. <https://doi.org/10.1080/19392699.2024.2398525> (2024).

26. Wang, Z. et al. Experimental study on geometric parameters of pore structure and quantitative evaluation of complexity of pulverized coal with different metamorphic degrees[J]. *Adv. Powder Technol.* **6** (8), 5865–5877. <https://doi.org/10.1016/j.apt.2022.103764> (2022).
27. Li, T. Wu Jianjun, Wang Xing-gang, Huang Hai. Particle size effect and temperature effect on the pore structure of low-rank coal[J]. *ACS Omega.* **6** (8), 5865–5877. <https://doi.org/10.1021/acsomega.0c06280> (2021).
28. Hu Biao. et al. Effect of pulverization on the microporous and ultramicroporous structures of coal using low-pressure CO<sub>2</sub> adsorption[J]. *Energy Fuels*, **33**(11), 10611–10621. <https://doi.org/10.1021/acs.energyfuels.9b02354> (2019).
29. Hu Biao. et al. Effects of equilibrium time and adsorption models on the characterization of coal pore structures based on statistical analysis of adsorption equilibrium and disequilibrium data[J]. *Fuel*, **281**, 118770. <https://doi.org/10.1016/j.fuel.2020.118770> (2020).
30. Jin, K. et al. Experimental investigation of pore structure damage in pulverized coal: implications for methane adsorption and diffusion characteristics[J]. *Energy Fuels*. **30** (12), 10383–10395. <https://doi.org/10.1021/acs.energyfuels.6b02530> (2016).
31. Cloke, M., Lester, E. & Belghazi, A. Characterisation of the properties of size fractions from ten world coals and their Chars produced in a drop-tube furnace[J]. *Fuel* **81** (5), 699–708. [https://doi.org/10.1016/S0016-2361\(01\)00162-4](https://doi.org/10.1016/S0016-2361(01)00162-4) (2002).
32. Lowell, S., Shields, J., Thomas, M. & Matthias, T. Characterization of porous solids and powders: surface area, pore size and density[M]. *J. Am. Chem. Soc.* **127** (40), 14117. <https://doi.org/10.1021/ja041016i> (2005).
33. Hou, S. et al. Pore structure characterization of low volatile bituminous coals with different particle size and tectonic deformation using low pressure gas adsorption[J]. *Int. J. Coal Geol.* **183**, 1–13. <https://doi.org/10.1016/j.coal.2017.09.013> (2017).
34. Hu Biao. et al. Experimental study on influence of adsorption equilibrium time on methane adsorption isotherm and Langmuir parameter[J]. *Advanced Powder Technology*, **32**(11), 4110–4119. <https://doi.org/10.1016/j.apt.2021.09.015> (2021)
35. Yi Minhao. et al. Effect of particle size and adsorption equilibrium time on pore structure characterization in low pressure N<sub>2</sub> adsorption of coal: an experimental study[J]. *Advanced Powder Technology*, **31**(10), 4275–4281. <https://doi.org/10.1016/j.apt.2020.09.004> (2020).
36. Mastalerz, M., Hampton, L. B., Drobnik, A. & Loope, H. Significance of analytical particle size in low-pressure N<sub>2</sub> and CO<sub>2</sub> adsorption of coal and shale[J]. *Int. J. Coal Geol.* **178**, 122–131. <https://doi.org/10.1016/j.coal.2017.05.003> (2017).
37. Dubinin, M. M. The potential theory of adsorption of gases and vapors for adsorbents with energetically nonuniform surfaces[J]. *Chem. Rev.* **60** (2), 235–241. <https://doi.org/10.1021/cr60204a006> (1960).
38. Everett, D. H. & Powl, J. C. Adsorption in slit-like and cylindrical micropores in the Henry's law region. A model for the microporosity of carbons[J]. *J. Chem. Soc. Faraday Trans.* **72**, 619–636. <https://doi.org/10.1039/F19767200619> (1976).
39. HORVÁTH, G. Z. A. Kawazoe K. Method for the calculation of effective pore size distribution in molecular sieve carbon[J]. *J. Chem. Eng. Jpn.* **16** (6), 470–475. <https://doi.org/10.1252/jcej.16.470> (2006).
40. Haghghatju, F. H. & Rafsanjani, Esmaeilzadeh, F. Estimation of the dimension of micropores and mesopores in single walled carbon nanotubes using the method Horvath-Kawazoe, Saito and Foley and BJH equations[J]. *Micro Nano Lett.* **12** (1), 1–5. <https://doi.org/10.1049/mnl.2016.0306> (2017).
41. Leofanti, G., Padovan, M., Tozzola, G. & Venturelli, B. Surface area and pore texture of catalysts[J]. *Catal. Today.* **41** (1), 207–219. [https://doi.org/10.1016/S0920-5861\(98\)00050-9](https://doi.org/10.1016/S0920-5861(98)00050-9) (1998).
42. Do, D. D. & Do, H. D. Modeling of adsorption on nongraphitized carbon surface: GCMC simulation studies and comparison with experimental data[J]. *The journal of physical chemistry, B. Condensed matter, materials, surfaces, interfaces & biophysical*, **110** (35), 17531–17538. <https://doi.org/10.1021/jp062386r> (2006).
43. Panagiotopoulos, A. Z. Direct determination of phase coexistence properties of fluids by Monte Carlo simulation in a new ensemble[J]. *Mol. Phys.* **100** (1), 237–246. <https://doi.org/10.1080/00268978700101491> (2002).
44. Angulo, R. F., Alvarado, V. & Gonzalez, H. Fractal dimensions from mercury intrusion capillary tests[C]. *SPE Latin America Petroleum Engineering Conference*, (Caracas, Venezuela, 1992). <https://doi.org/10.2523/23695-ms>
45. Airey, E. M. Gas emission from broken coal. An experimental and theoretical investigation[J]. *Int. J. Rock. Mech. Min. Sci. Geomech. Abstracts.* **5** (6), 475–494. [https://doi.org/10.1016/0148-9062\(68\)90036-3](https://doi.org/10.1016/0148-9062(68)90036-3) (1968).

## Author contributions

Biao Hu: Data curation, Formal analysis, Funding acquisition, Methodology, Project administration, Resources, Writing - review and editing. Zeyu Ren: Data curation, Formal analysis, Methodology, Validation, Writing - original draft. Rongwei Luo: Investigation, Validation. Shugang Li: Conceptualization, Methodology, Resources. Rong Zhang: Investigation, Validation, Writing - review and editing. Hang Long: Data curation, Formal analysis, Writing - review and editing. Liang Cheng: Formal analysis, Methodology. All authors have read and agreed to the published version of the manuscript.

## Funding

Open access funding provided by the National Natural Science Foundation of China (No. 52304255, 52304276), the Excellent Youth Program of Xi'an University of Science and Technology (No. 2024YQ3-15), the Shaanxi Province Postdoctoral Science Foundation (No. 2023BSHYDZZ153).

## Declarations

## Competing interests

The authors declare no competing interests.

## Declaration of competing interest

The authors declare that they have no known competing financial interests or personal relationships that could have appeared to influence the work reported in this paper.

## Additional information

**Correspondence** and requests for materials should be addressed to B.H.

**Reprints and permissions information** is available at [www.nature.com/reprints](http://www.nature.com/reprints).

**Publisher's note** Springer Nature remains neutral with regard to jurisdictional claims in published maps and institutional affiliations.

**Open Access** This article is licensed under a Creative Commons Attribution-NonCommercial-NoDerivatives 4.0 International License, which permits any non-commercial use, sharing, distribution and reproduction in any medium or format, as long as you give appropriate credit to the original author(s) and the source, provide a link to the Creative Commons licence, and indicate if you modified the licensed material. You do not have permission under this licence to share adapted material derived from this article or parts of it. The images or other third party material in this article are included in the article's Creative Commons licence, unless indicated otherwise in a credit line to the material. If material is not included in the article's Creative Commons licence and your intended use is not permitted by statutory regulation or exceeds the permitted use, you will need to obtain permission directly from the copyright holder. To view a copy of this licence, visit <http://creativecommons.org/licenses/by-nc-nd/4.0/>.

© The Author(s) 2025